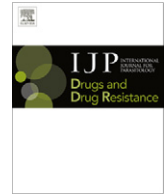




Contents lists available at SciVerse ScienceDirect

# International Journal for Parasitology: Drugs and Drug Resistance

journal homepage: [www.elsevier.com/locate/ijpddr](http://www.elsevier.com/locate/ijpddr)

## Brief Report

### *Teladorsagia circumcincta*: Molecular characterisation of the avr-14B subunit and its relatively minor role in ivermectin resistance

María Martínez-Valladares<sup>a,\*</sup>, Peter Geldhof<sup>b</sup>, Nicholas Jonsson<sup>c</sup>, Francisco A. Rojo-Vázquez<sup>a,d</sup>, Philip Skuce<sup>e</sup>

<sup>a</sup> Instituto de Ganadería de Montana (CSIC-ULE), Finca de Marzanas, 24346 Grulleros, León, Spain

<sup>b</sup> Department of Virology, Parasitology and Immunology, Faculty of Veterinary Medicine, Ghent University, Salisburylan 133, 9820 Merelbeke, Belgium

<sup>c</sup> School of Veterinary Medicine, College of Medical, Veterinary & Life Sciences, University of Glasgow, 464 Bearsden Road, Glasgow G61 1QH, UK

<sup>d</sup> Faculty of Veterinary Medicine, University of León, Campus de Vegazana, 24071 León, Spain

<sup>e</sup> Moredun Research Institute, Pentlands Science Park, Bush Loan, Penicuik, Edinburgh EH26 0PZ, UK

## ARTICLE INFO

### Article history:

Received 1 February 2012

Received in revised form 27 March 2012

Accepted 29 March 2012

Available online 17 April 2012

### Keywords:

*Teladorsagia circumcincta*

Sheep

Anthelmintic resistance

Ivermectin

GluCl channels

## ABSTRACT

Individual mutations (e.g. L256F) and polymorphisms in the avr-14B gene, a glutamate-gated chloride channel subunit, have been associated with ivermectin (IVM) resistance in *Caenorhabditis elegans* and *Cooperia oncophora*. The aim of the present study was to determine the full-length coding sequence of the avr-14B subunit homologue in *Teladorsagia circumcincta* and determine the presence/absence of the putative L256F SNP or any other potential SNPs of interest. Subsequently, we investigated sequence polymorphisms and transcription patterns between four different *T. circumcincta* isolates: two from Scotland (MTci1 susceptible and MTci5 triple resistant to benzimidazoles, levamisole and IVM) and two from Spain (S-Sp susceptible and R-Sp double resistant to levamisole and IVM). The complete amino acid sequence of the *T. circumcincta* avr-14B subunit comprises 438 amino acids. Pyrosequencing analysis failed to detect the presence of the L256F mutation in any of the MTci5 or Sp-R samples tested. However, we revealed significant allele frequency changes by means of SSCP analysis of a 106 bp region encompassing the L256F SNP. Allele E showed the greatest change, following IVM exposure *in vitro* and *in vivo*, although sequence analysis did not reveal any coding changes. Sequence analysis of the full-length avr-14B coding sequence showed that two SNPs exclusively found in the resistant strain MTci5 (I270F and T305A) are situated in codons involved in the interaction of the receptor with IVM. Moreover, other potentially significant SNPs (K361E and L364M) were identified between transmembrane regions 3 and 4. However, due to the low frequency of all these SNPs, we cannot conclude they confer IVM resistance in *T. circumcincta*. Moreover, a modest increase in expression of the avr-14B in both resistant isolates has been shown although these differences were not sufficiently great to consider avr-14B to be the sole or even a major determinant of IVM resistance in this species.

© 2012 Australian Society for Parasitology Published by Elsevier Ltd. All rights reserved.

## 1. Introduction

The gastrointestinal nematode, *Teladorsagia circumcincta*, is the predominant parasite of grazing small ruminants in temperate parts of the world. This parasite contributes significantly to parasitic gastroenteritis and causes considerable economic losses due to effects on appetite and weight gain, alongside the cost of treating infected animals. The control of teladorsagiosis is carried out almost entirely by strategic application of broad-spectrum anthelmintics. These belong mainly to three chemical classes, namely the benzimidazoles (BZs), imidazothiazoles (e.g. levamisole, LEV) and macrocyclic lactones (MLs). Recently, a fourth chemical class, the

amino-acetonitrile derivatives (AADS, e.g. monepantel) has been introduced onto the sheep market in parts of the Southern Hemisphere and Europe (Kaminsky et al., 2009). However, over-use or misuse of existing drugs in the past has resulted in the development of anthelmintic resistance (Prichard, 1994), which is now a serious problem for the livestock industry worldwide. One of the most effective anthelmintics to control infection by *T. circumcincta* in sheep is ivermectin (IVM), an avermectin and member of the ML family. ML anthelmintics inhibit movement and feeding by affecting the body wall and pharyngeal musculature, leading to paralysis and death of susceptible parasites. The mode of action of the avermectins is thought to involve interaction with invertebrate glutamate-gated chloride channels, or GluClS (Cully et al., 1994), located in the parasite's neuromuscular system. In the free-living model nematode, *Caenorhabditis elegans*, IVM

\* Corresponding author. Tel.: +34 987 317 064; fax: +34 987 317 161.

E-mail address: [mmarva@unileon.es](mailto:mmarva@unileon.es) (M. Martínez-Valladares).

activates different  $\alpha$  subunits of GluCl channels encoded by *avr-14*, *avr-15*, *glc-1* and *glc-3* genes, respectively (Dent et al., 1997, 2000; Horoszok et al., 2001). As a result, these genes are widely considered to be prime candidate IVM resistance genes. The *avr-14* and *avr-15* genes are alternatively spliced, giving two subunits each, A and B (Dent et al., 1997; Laughton et al., 1997). The *avr-14* subunit has been described and studied in various free-living and parasitic nematodes, such as *C. elegans* (Cully et al., 1994), *Haemonchus contortus* (McCavera et al., 2009), *Cooperia oncophora* (Njue and Prichard, 2004), *Ascaris suum* (Jagannathan et al., 1999), cyathostomins (Tandon et al., 2006), *Dirioflaria immitis* (Yates and Wolstenholme, 2004), and also reviewed by McCavera et al. (2007) detailing the specific nomenclature for each species. The subunits A and B share the N-terminal ligand-binding domain but differ in their C-terminal channel-forming domains. When the *avr-14B* subunit was expressed in *Xenopus* oocytes, it formed functional channels where the normal ligand, L-glutamate, and IVM could bind (Dent et al., 2000), however, this response was not observed with the *avr-14A* subunit. Individual mutations and polymorphisms in *avr-14* subunits have been associated with IVM resistance in *C. elegans* as well as in the cattle parasite *C. oncophora* (Dent et al., 2000; Njue et al., 2004). In the latter study, investigating an IVM resistant *C. oncophora* field isolate, three single nucleotide polymorphisms (SNPs)-E114G, V235A, L256F – were described in the N-terminal extracellular domain of the *avr-14B* subunit (Njue et al., 2004). With the aim of determining whether these mutations contribute to loss of L-glutamate and IVM sensitivity, alleles carrying the respective SNPs were cloned and expressed in *Xenopus* oocytes. Whole-cell 2-electrode voltage-clamp recordings showed that only the L256F polymorphism was functionally active, causing a 3.2 and 2.6-fold loss of sensitivity to L-glutamate and IVM, respectively (Njue et al., 2004). Recently, Ghosh et al. (2012) reported a naturally occurring four-amino-acid deletion in the ligand-binding domain of *glc-1*, the alpha-subunit of a glutamate-gated chloride channel, confers resistance to avermectins in the model nematode *C. elegans*.

The aim of the present study, therefore, was to identify and characterize, for the first time, the *avr-14B* subunit in *T. circumcincta* and to determine the presence/absence of the putative L256F SNP or any other potential SNPs of interest. Subsequently, we investigated sequence polymorphisms and transcription patterns between *T. circumcincta* isolates of known IVM resistance status.

## 2. Materials and methods

### 2.1. *T. circumcincta* populations

Four *T. circumcincta* isolates were used in this study, two from Scotland and two from Spain. The Scottish populations were: MTc1, which was isolated from lambs on a Midlothian farm in 1979, prior to the introduction of LEV and ML anthelmintics and shown by egg hatch test (EHT) to be BZ susceptible (D. Bartley, personal communication); and MTc5, which was also isolated in Scotland and is triple resistant to BZ, LEV and IVM, 59, 88 and 60%, respectively, as determined by faecal egg count reduction tests (FECRT) (Bartley et al., 2004). The Spanish populations were both isolated in Leon province; the first (S-Sp) is susceptible to BZ, LEV and IVM, whereas the second (R-Sp) is double resistant to LEV and IVM, 58% and 88%, respectively, after FECRT (Martínez-Valladares et al., 2012).

With the isolate MTc5 we carried out a selection after the *in vitro* test, larval feeding inhibition assay (LFIA) (Álvarez-Sánchez et al., 2005), by establishing a discriminating dose to identify the top 5% of larvae capable of feeding at the highest IVM concentrations,

and *in vivo* through analysis of adults surviving a therapeutic dose of IVM treatment (0.2 mg/kg), according to the manufacturer's recommendations (Ivomec, Merial).

### 2.2. Extraction of nematode RNA

For total RNA extraction, 20,000 L3 or a pool of mixed sex adult worms was collected from the respective isolates as a pellet and 200  $\mu$ l of lysis buffer (10 mM Tris-HCl pH 7.5 + 0.5% SDS + 10 mM EDTA + 5% mercaptoethanol) added. The pellet was then incubated overnight at  $-80^{\circ}\text{C}$ , followed by 3 freeze-thaw cycles ( $-80^{\circ}\text{C}$ /room temperature). Larvae were incubated with proteinase K (0.5 mg/ml) for 1 h at  $55^{\circ}\text{C}$  and later crushed with a tissue grinder. The pool was lysed in 1 ml of TRIzol<sup>®</sup> according to manufacturer's recommendations (Invitrogen). The RNA pellet was air dried for 10 min at room temperature then dissolved in 657  $\mu$ l diethyl pyrocarbonate (DEPC) water. For DNase treatment, 9  $\mu$ l RNase inhibitor, 9  $\mu$ l DNase and 75  $\mu$ l 10 $\times$  buffer were added to the RNA solution. The sample was incubated at  $37^{\circ}\text{C}$  for 30 min and then 750  $\mu$ l of phenol:chloroform (from a 1:1 phenol:chloroform mixture) was added and mixed vigorously. The RNA solution was centrifuged at 1230 g for 8 min, at  $4^{\circ}\text{C}$ , and the aqueous phase transferred to a fresh RNase-free tube to precipitate the RNA by adding an equivalent volume of isopropanol. The sample was then incubated at room temperature for 10 min and centrifuged at 12,300 g for 10 min, at  $4^{\circ}\text{C}$ . The supernatant was removed and 900  $\mu$ l ethanol added to wash the pellet. The sample was again centrifuged at 12,300 g for 5 min, at  $4^{\circ}\text{C}$ . The pellet was dried for 10 min at room temperature and then dissolved in an appropriate volume of DEPC water. The RNA concentration was measured with a NanoDrop ND-1000 spectrophotometer (NanoDrop Technologies, Wilmington, DE, USA).

### 2.3. Generation of the full-length *avr-14B* coding sequence

A one-step Reverse Transcriptase protocol was used to amplify the full-length *T. circumcincta* *avr-14B* cDNA sequence from the susceptible Moredun isolate, Mtci1, to generate a baseline consensus sequence. First-strand cDNA synthesis was carried out by using 1  $\mu$ g of total RNA and following the manufacturer's protocol (Invitrogen). PCR primers were designed based on sequence alignment of available *avr-14B* orthologous genes from *Ostertagia ostertagi* (FR690075), *C. oncophora* (AY372756), *H. contortus* (Y14234), *C. elegans* (U41113), *D. immitis* (AJ581673) and *A. suum* (Y18347) (Supplementary Table S1 and Fig. S1). Primer SL1 was based on the spliced leader 1 sequence (Blaxter et al., 1998). PCR conditions to amplify each fragment comprised a 2 min denaturation and polymerase activation step at  $95^{\circ}\text{C}$ , 35 cycles of  $95^{\circ}\text{C}$  for 30 s,  $x^{\circ}\text{C}$  (annealing temperature for specific primers) for 30 s and  $72^{\circ}\text{C}$  for 45 s and one final elongation step at  $72^{\circ}\text{C}$  for 10 min. Specific PCR products were visualized on a 1.5% agarose gel stained with ethidium bromide. Bands were then purified (GeneClean<sup>®</sup>), PCR products ligated into a p-GEMT-Easy vector (Promega) and cloned into DH5 $\alpha$  cells. Afterwards, positive clones were sequenced in both directions using the universal primers SP6 and T7. Alignment and analysis of the partial sequences were carried out with the DNASTAR software program (DNASTAR INC).

A fragment of almost the full-length transcript, 1163 bp, was subsequently amplified in a single reaction with primers F4 and R4 (Supplementary Table S1), again using cDNA from the susceptible isolate, Mtci1. PCR conditions to amplify this fragment comprised a 2 min denaturation and polymerase activation step at  $95^{\circ}\text{C}$ , 35 cycles of  $95^{\circ}\text{C}$  for 30 s,  $x^{\circ}\text{C}$  (annealing temperature for specific primers) for 30 s and  $72^{\circ}\text{C}$  for 1 min 30 s and one final elongation step at  $72^{\circ}\text{C}$  for 10 min. PCR products were analysed as described previously.

#### 2.4. Analysis of the full-length *avr-14B* coding sequence

With the aim of investigating the extent of polymorphism in the full-length *avr-14B* sequence, two pairs of primers, F1/R1\_snp and F2/R2\_snp (Supplementary Table S1) were designed to amplify two fragments of 753 and 688 bp, each, to cover the complete coding sequence. cDNA was synthesised from pools of L3 from the respective susceptible and resistant isolates, in this case MTci1 and MTci5 and Sp-S and Sp-R. PCR conditions to amplify each fragment were the same as described in Section 2.3. PCR products were cloned into the pGEM-T (Qiagen) vector system for subsequent sequence analysis. At least 15 clones from each pair of primers were sequenced. Moreover, all sequences analyzed with other pairs of primers are included in the results.

#### 2.5. Pyrosequencing analysis of the putative L256F SNP

A Pyrosequencing assay was designed, using the proprietary assay design software (Biotage, Sweden) with the aim of investigating the presence/absence of the L256F polymorphism previously associated with IVM resistance in *C. oncophora* (Njue and Prichard, 2004). Template DNA, extracted from individual L3 or pools of >10,000 L3, from the resistant MTci5 isolate was used as template, essentially as described by Skuce et al. (2010). Briefly, the same flanking PCR primer set as employed for SSCP analysis was used for Pyrosequencing (Supplementary Table S1), except that the forward primer was biotinylated for subsequent template purification, and a sequencing primer (antisense) (L256FSeq) was designed to target the putative CTC to CTT mutation representing the L256F SNP (primers used are shown in Supplementary Table S1). PCR conditions used were 94 °C for 10 min followed by 40 cycles of 94 °C for 30 s, 55 °C for 30 s and 72 °C using NovaStart Hot Start Master Mix as in standard PCR, with the exception that the final concentration of the biotinylated primer was reduced to 0.2 μM to avoid interference with subsequent Pyrosequencing template preparation. Pyrosequencing assays were performed on a Biotage PyroMark ID machine (Qiagen), according to manufacturer's recommendations. Following PCR amplification, 37 μl 2× Binding Buffer (Biotage) and 3 μl streptavidin–Sepharose beads (Roche) were subsequently added to each 40 μl PCR product and the solution agitated for 5 min to allow binding of biotinylated PCR products to the beads. Single-stranded template DNA was isolated using the designated Vacuum Prep Tool (Biotage) and added to 40 μl sequencing primer in annealing buffer in a 96 well microplate. The sequencing primer was allowed to anneal to the respective templates and samples were run in either genotyping mode (for individual L3 lysates) or allele quantification mode (for pooled material), alongside sequencing primer ± biotinylated primer only controls.

#### 2.6. Single strand conformation polymorphism (SSCP) analysis

SSCP was employed to investigate *avr-14B* sequence polymorphism within and between the different *T. circumcincta* isolates, MTci1, MTci5, MTci5 after the selection with IVM and MTci5 post-LFIA. The selection of MTci5 is described in Section 2.1.

PCR primers (F\_sscp and R\_sscp) were designed to amplify a 106 bp polymorphic region of the coding sequence, encompassing the putative L256F SNP (Supplementary Table S1). The *T. circumcincta* isotype-1 β-tubulin gene was employed as a control for SSCP analysis of MTci1 and MTci5, using primers described in Skuce et al. (2010). PCR products were subjected to SSCP, essentially as described by Blackhall et al. (1998, 2008). Briefly, 5 μl aliquots of PCR products generated from individual L3 were heat denatured for 5 min at 95 °C in SSCP loading buffer (95% formamide, 10 mM NaOH, 0.25% bromophenol blue and 0.25% xylene cyanol) and

quenched rapidly on ice. A 20% (37.5:1) polyacrylamide:bisacrylamide (Severn Biotech, UK) gel mixture in 1× TBE buffer (0.045 M Tris–borate; 0.001 M EDTA, pH 8.0) proved to give optimal resolution. 5 μl aliquots of PCR products from individual L1 larvae were loaded on gels and subjected to vertical electrophoresis at a constant voltage of 120 V for 18 h. Following electrophoresis, gels were soaked in GelRed solution (Biotium Inc., CA, USA) in preparation for scanning under UV in a BioRad FX Molecular Imager scanner. Individual alleles were identified, based on their respective electrophoretic patterns (Fig. 1A). PCR products from designated homozygous individuals were subsequently cloned into the pGEM-T vector system (Promega) for sequencing. At least 5 clones of each genotype were sequenced. Allele counts and genotypes from the four populations under test (MTci1, MTci5, MTci5-post-IVM and MTci5 post-LFIA) were subjected to population genetic analysis using Genalex and Genepop software.

#### 2.7. Semi-quantitative PCR and Real-Time PCR

A two-step semi-quantitative reverse transcriptase (RT)-PCR method was used to measure *avr-14B* gene expression. One microgram of total RNA was reverse transcribed using the iScript cDNA Synthesis Kit (BioRad). The resulting cDNA was then amplified by PCR using the GoTaq DNA Polymerase (Promega). Concentrations of cDNA for the four isolates were normalized against the actin gene using the primers described in Supplementary Table S2, which were designed based on the nucleotide sequence under accession number BG734306. PCR conditions to amplify the actin gene comprised of a 2 min denaturation and polymerase activation step at 95 °C, 33 cycles of 95 °C for 30 s, 63 °C for 30 s and 72 °C for 45 s and one final elongation step at 72 °C for 10 min. The amplification of the *avr-14B* gene was carried out with the primers described at Supplementary Table S2. PCR conditions consisted of 2 min denaturation step at 95 °C, 37 cycles of 95 °C for 30 s, 60 °C for 30 s and 72 °C for 45 s and an elongation step at 72 °C for 10 min. PCR products were analyzed by electrophoresis on 1.5% agarose gels.

A quantitative Real-Time PCR using SYBR® green detection was designed and optimized for *avr-14B* transcript profiling, using two commonly employed housekeeping genes as controls, actin and GAPDH (glyceraldehyde 3-phosphate dehydrogenase). Real-time analysis was carried out on a StepOnePlus Real-Time PCR system (Applied Biosystems). PCR amplification mixtures (25 μl) contained 2 μl cDNA, 12.5 μl Master Mix (SYBR® Green PCR Master Mix, Applied Biosystems) and 400 nM forward and reverse primers. *T. circumcincta*-specific actin and GAPDH primers were designed based on the nucleotide sequence accession numbers BG734306 and AJ000064, respectively (Supplementary Table S2). The cycling conditions comprised a 10 min denaturation and polymerase activation step at 95 °C, 40 cycles of 95 °C for 15 s, 63 °C for 30 s and 72 °C for 30 s. Upon completion of the amplification program, a dissociation analysis (52–95 °C) was performed to determine the purity of the PCR amplicons. To estimate amplification efficiencies, a standard curve was generated for each primer pair based on known quantities of cDNA. The experiments were performed in triplicate. All assays included a standard curve, a no-template control and each of the test cDNAs.

Raw Ct values obtained after Real-Time PCR were transformed to concentrations using the comparative Ct method and specific PCR efficiencies by the geNorm application (Vandesompele et al., 2002; Van Zeveren et al., 2007) which was downloaded from <http://www.medgen.ugent.be/~jvdesomp/genorm/>. Differential gene expression was considered significant when the 95% confidence interval of the mean normalized expression levels did not overlap (equivalent to  $p < 0.05$ ).

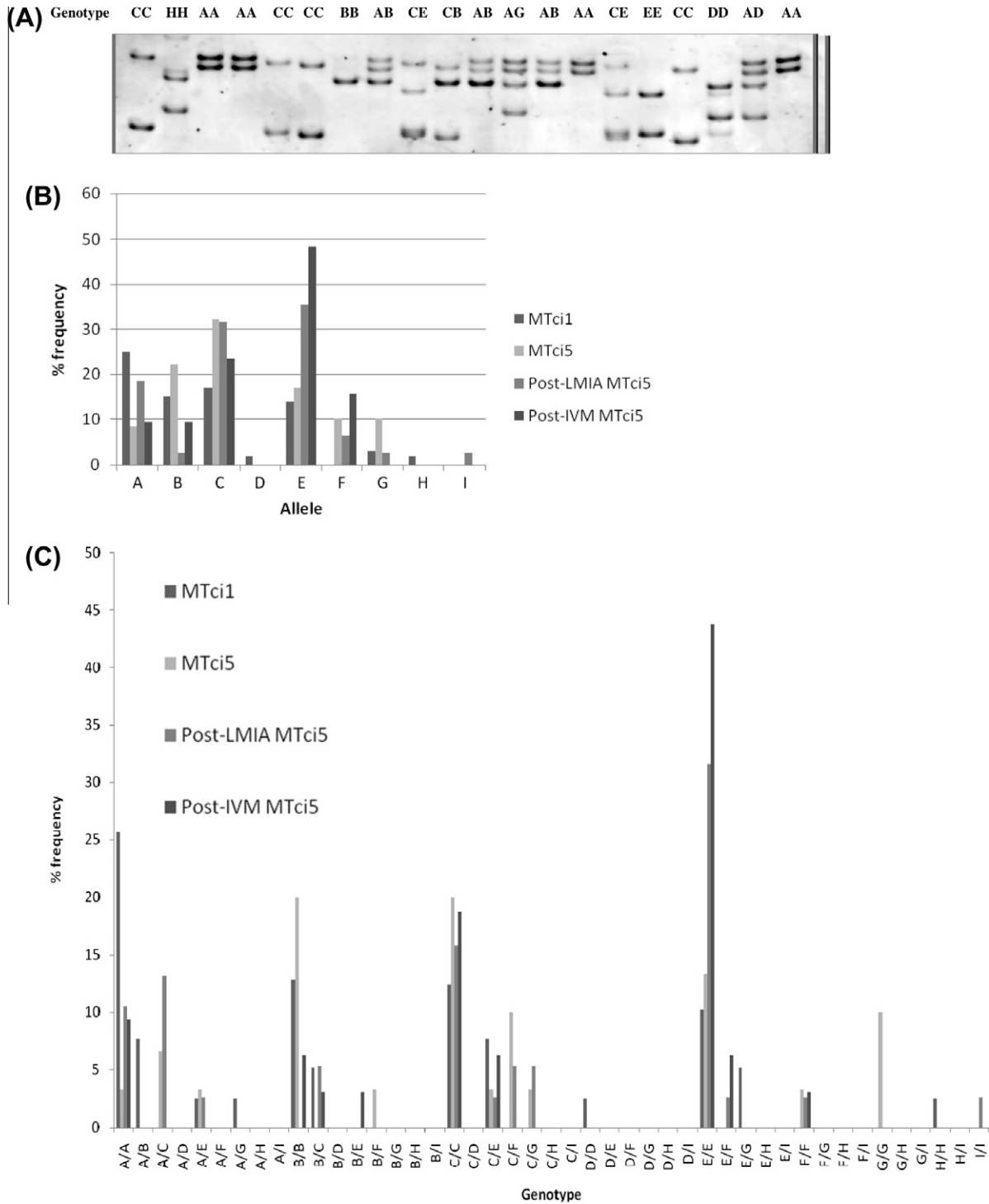


**Fig. 1.** Single strand conformation polymorphism (SSCP) analysis of the *T. circumcincta* avr-14B locus. A: Representative SSCP profile and associated genotypes from 20 individual L1 larvae from the MTci1 population. B: SSCP allele frequency profiles for the 4 *T. circumcincta* populations under investigation, namely MTci1, MTci5, post-LMIA MTci5 and post-IVM MTci5. C: SSCP genotype frequency profiles for the 4 *T. circumcincta* populations under investigation, namely MTci1, MTci5, post-LMIA MTci5 and post-IVM MTci5.

**3. Results and discussion**

Here we report, for the first time, the coding sequence of the avr-14B subunit from *T. circumcincta* and an investigation into its sequence polymorphism and transcription pattern between isolates of known IVM resistance status. The nucleotide sequence described in this paper for the avr-14B subunit in *T. circumcincta*

comprises 1410 bp in total, including the spliced leader sequence, SL1. The SL1 primer, 21 bp, was followed by a 72 bp 5' untranslated region before the beginning of the coding sequence. The complete amino acid sequence of the avr-14B subunit comprises 438 amino acids (Genbank accession number:JQ946071) and possesses characteristic features of the ligand-gated ion channel super-family. These channels belong to the Cys-loop receptor family and are

critical not only for maintaining appropriate neuronal activity, but also as the accepted therapeutic targets for a number of drugs (e.g. benzodiazepines and anaesthetics), including IVM (Thompson et al., 2010). This receptor consists of five subunits each comprising a large N-terminal extracellular domain of mostly  $\beta$ -sheet structure, followed by four  $\alpha$ -helical TM regions; these TM helices adopt a fold with the five TM2 segments lining the pore and adopting an open channel conformation (Hibbs and Gouaux, 2011). Within the *T. circumcincta* sequence are present the signature pair of cysteine residues within the N-terminal region at positions 178 and 192, another different pair of cysteine residues, characteristic of GluCl and glycine receptors, at positions 239 and 250 and four proposed transmembrane regions (TM1–4) in the C-terminal region. The TM regions were located between the amino acid positions 262 (S) – 285 (L) for TM1, 291 (P) – 310 (G) for TM2, 325 (D) – 347 (Y) for TM3 and 407 (R) – 430 (A) for TM4. The protein similarity between the avr-14B subunit in *T. circumcincta* and other species is 98% with *O. ostertagi* (CBX19419), 96% with *C. oncophora* (AAR21855), 95% with *H. contortus* (CAA74623), 82% with *C. elegans* (AAC25482), 74% with *D. immitis* (CAE46430) and 69% with *A. suum* (Supplementary Fig. S2). With the aim of investigating the presence of mutations associated with IVM resistance, two cDNA fragments were amplified and cloned individually from pools of L3 from the respective susceptible and resistant isolates, MTci1 and MTci5 and Sp-S and Sp-R. Both fragments included the complete coding sequence. A total of 56 coding SNPs were identified overall (Table 1). However, most of these were only present in one clone, probably as artefacts generated during the amplification. The most prevalent clones were found in the Scottish populations: S282P (5/15) and R32G (4/15) in McTi1 and K361E (8/27), I270 (7/33) and L364M (5/27) in McTi5. This low allele frequency was also shown by subsequent examination of sequence chromatograms from pooled L3 samples (data not shown). Occasionally, two of these SNPs were found in the same clone (data not shown). Two SNPs found in this study, I270F and T305A, are situated on the TM1 and TM2 regions, and were only described in the resistant strain McTi5. Recently, the first three-dimensional (3D) structure of the

homopentameric *C. elegans* GluCl channel  $\alpha$ 1 subunit (glc-1) has been resolved by means of a crystal structure (Hibbs and Gouaux, 2011). Comparing the avr-14B subunit from *T. circumcincta* with this 3D structure, the I270F and T305A SNPs are situated in codons involved in the interaction of the receptor with IVM by means of Van der Waals forces. Therefore, the substitution of the amino acids in these specific positions could cause the incorrect binding of IVM although the frequencies of both SNPs were low, particularly for T305A (2 out of 29 clones). IVM is bound at subunit interfaces on the periphery of the TM regions, next to the extracellular side of the membrane bilayer. Wedged between the TM3  $\alpha$ -helix on the principal subunit and the TM1  $\alpha$ -helix on the complementary subunit, IVM interacts with the pore lining of the TM2 region of the principal subunit and the TM2–3 loop (Hibbs and Gouaux, 2011). As a result, it can be proposed that polymorphisms present on the TM1–3 regions and TM2–3 loop will probably be more involved in the development of IVM anthelmintic resistance than those described on the large N-terminal extracellular domain. In the case of *Drosophila*, mutations that confer resistance to IVM in both GABA and GluCl receptors are in, or very close to, the TM2 region, suggesting that this part of the receptor is a potential “hot-spot” for resistance-associated polymorphisms (McCavera et al., 2007). It is worth noting that other SNPs, found also in the resistant isolate McTi5, K361E and L364M, are located on the TM3–4 loop, between the TM3–4 regions. In the glycine receptor  $\alpha$  subunits, also belonging to Cys-loop receptor family, the cytoplasmic TM3–4 loop carries motifs for phosphorylation (Harvey et al., 2004), ubiquitination (Büttner et al., 2001), as well as putative Ca<sup>2+</sup>-dependent intracellular factors (Fucile et al., 2000), and a basic cluster thought to ensure correct transmembrane topology (Sadler et al., 2003). For these reasons, SNPs located in this region could be related to a lower dose-response to IVM administration. However, again, due to the low frequency of the respective SNPs found in the current study – I270 (7/33), T305A (2/29), K361E (8/27) and L364M (5/27) – and the absence of any electrophysiological demonstration of a functional role, we cannot conclude they confer IVM resistance in *T. circumcincta*. It is important to note that the development

**Table 1**  
SNPs described in the coding sequence of the avr-14B gen and number of sequences analyzed (number of sequences with the SNP/total number of sequences analyzed).

SNPs	S-Sp	R-Sp	McTi1	McTi5	Situation in the 3D structure	SNPs	S-Sp	R-Sp	McTi1	McTi5	Situation in the 3D structure
I11L	2/15	–	–	–		W284R	–	1/25	–	–	TM1
S26T	1/15	–	–	–		P291L	–	1/25	–	–	TM2
R32G	–	–	4/15	–		V294I	–	–	–	1/33	TM2
I73T	–	–	–	1/15	$\beta$ 1 Sheet	T303A	–	–	–	1/29	TM2
L75F	–	–	–	2/15	$\beta$ 1 Sheet	T305A	–	–	–	2/29	TM2
S79P	–	–	–	1/15		G310D	–	–	–	1/29	TM2
N85D	1/15	–	–	–		L315P	–	–	–	1/29	TM2–3 loop
E111R	–	–	–	1/15		P316L	–	1/25	–	–	TM2–3 loop
F108L	–	1/15	–	–		V326A	–	–	–	1/29	TM3
V119A	1/15	–	–	–		C331R	–	1/25	–	–	TM3
A146T	1/15	–	–	–		F334L	–	1/25	–	–	TM3
K162E	1/15	1/15	–	–		I335T	–	–	2/15	–	TM3
S173F	1/15	–	–	–		F336S	–	–	–	1/29	TM3
C178Y	–	–	3/15	–	$\beta$ 6 Sheet, Cys loop	K351E	1/15	1/25	–	–	TM3–4 loop
T202A	1/15	–	–	–		R355C	–	1/25	–	–	TM3–4 loop
E230G	–	–	–	4/29		K358E	–	–	2/15	–	TM3–4 loop
Q232R	–	1/25	–	–		K361E	–	–	–	8/27	TM3–4 loop
Y248C	–	1/25	–	–		T362A	–	1/25	–	–	TM3–4 loop
R252W	1/15	–	–	–		L364M	–	–	–	5/27	TM3–4 loop
K254E	–	–	–	1/33		E372G	1/15	–	–	–	TM3–4 loop
R258Q	–	–	–	1/33		L404P	–	1/25	–	–	TM3–4 loop
Y264H	–	–	–	1/33	TM1	S405L	–	1/25	–	–	TM3–4 loop
L268P	–	2/25	–	–	TM1	S412A	–	–	–	1/19	TM4
I270F	–	–	–	7/33	TM1	S418F	–	–	–	1/18	TM4
M274T	1/15	–	–	–	TM1	F426L	1/15	–	–	–	TM4
S279L	–	–	–	1/33	TM1	Y427C	–	–	–	1/18	TM4
S282P	–	–	5/15	–	TM1	V429E	–	2/25	–	–	TM4
F283S	1/15	–	–	–	TM1	S435G	–	–	5/15	–	

of anthelmintic resistance could be related, not only with a unique SNP, but also with other SNPs in combination or haplotypes to produce the full phenotypic expression of resistance. Mes (2004) showed that polymorphism within a 1 Kb region of the subunit *avr-14A*, namely *gbr-2A* in *H. placei*, was essentially linked into a haplotype that segregated as an allele.

None of the *T. circumcincta* isolates carried the L256F SNP, putatively situated on the  $\beta$ 10 loop and related previously with IVM resistance in *C. oncophora* (Dent et al., 2000; Njue et al., 2004). Pyrosequencing analysis failed to detect the presence of the putative L256F mutation in any of the MTci5 or Sp-R samples tested, whether multiple individual L3 or pools of >10,000 L3. In the former, all samples tested ( $n > 200$ ) proved to have the susceptible genotype and were uniformly designated as C/C homozygotes. There was no evidence of any heterozygotes at this locus. Similarly, in allele quantification mode, the frequency of the putative susceptible allele in the pooled MTci5 and Sp-R samples was consistently 100%. McCavera et al. (2009) suggested that this SNP could be involved in mediating the allosteric properties of the receptor although it was unlikely to play a direct role in ligand binding. To date, the L256F SNP has not been described in resistant isolates of *H. contortus* (McCavera et al., 2009), nor in an experimentally selected *O. ostertagi* resistant isolate (El-Abdellati et al., 2011). El-Abdellati et al. (2011) did not find this mutation in a naturally selected *C. oncophora* resistant isolate from Belgium either.

On the other hand, the four populations under study by SSCP at the *avr-14B* locus (i.e. MTci1, MTci5, MTci5-post IVM and MTci5 post-LFIA) all displayed a high degree of allelic richness. Nine alleles were identified in total from the >30 individuals examined from each population (Fig. 1B and C). Allele A would appear to be the predominant allele in the susceptible MTci1 population (freq = 0.320). Allele E showed the greatest change across the three populations, increasing from approximately 0.179 (in both MTci1 and MTci5) to 0.355 in the selected population (MTci5 post-LFIA) and increasing further to 0.483 in the MTci5-post IVM population. The increase in frequency from MTci1 to MTci5 post-IVM was highly significant ( $\chi^2 = 17.9$ ,  $P < 0.001$ ). None of the populations proved to be in Hardy Weinberg equilibrium at the *avr-14B* locus, all showing a highly significant heterozygote deficiency ( $p < 0.001$ ). The strong heterozygote deficit in all populations was considered most likely to be a result of null alleles resulting from consistent PCR failure of one or more alleles. The potential role of a null allele was explored *post hoc* by creation of a dataset in which the presence of a single null allele was assumed within the susceptible MTci1 population (data not shown). Subsequent sequence analysis of the ~100 bp fragment used for SSCP revealed numerous allele-specific SNPs, none of which resulted in changes to the translated amino acid sequence. This does not preclude such changes being located elsewhere in the coding sequence or, indeed, in intervening non-coding regions. Significantly, we found no allele frequency changes in the control gene, isotype-1  $\beta$ -tubulin, following IVM exposure *in vitro* or survival *in vivo*, apart from the inherent differences between MTci1 and MTci5 prior to pressurisation, as reported in Skuce et al. (2010).

It has also been proposed that anthelmintic resistance could be associated with the expression level of genes implicated in the process (Wolstenholme et al., 2004). With the aim of confirming preliminary semi-quantitative PCR results (Supplementary Fig. S3), *avr-14B* gene expression was quantified by Real-Time PCR in pools of L3 from the four different isolates and in adults from the two Spanish isolates. The efficiencies of the Real Time PCR were uniformly high and ranged from 95% to 105%, making all assays suitable for quantitative analysis. All PCR assays generated a single band and the absence of primer dimer formation was confirmed by a dissociation curve analysis. In the current study, increased expression of the *avr-14B* in both *T. circumcincta*

resistant isolates, compared to their susceptible counterparts, has been shown by means of Real-Time PCR. After Real-Time PCR in L3 samples, the differences between resistant and susceptible populations were higher in the Scottish isolates (2.14-fold) than in the Spanish populations (1.75-fold) ( $p < 0.05$ ) (Fig. 2A). This most likely reflects the anthelmintic resistance status of the respective isolates, with the Scottish isolate being phenotypically the more resistant, at least as determined by FECRT (IVM efficacies of 60 and 88%, respectively). However, the geographic differences in the expression level of *avr-14B* must be taken into account jointly with the resistance status. Comparing the isolates from the different locations, the expression level of R-Sp was 1.48-fold higher than in McTi1; however, the *avr-14B* gene expression was 2.51-fold higher in MTci5 than in S-Sp ( $p < 0.05$ ). The fact that the expression levels were similar between a susceptible (MTci1) and resistant (R-Sp) isolate, most likely simply reflects the fact that the latter is only marginally resistant, as defined by FECRT. Regarding adult worms from the Spanish isolate, the expression level was higher in females than in males and, in both cases, in the resistant worms. In males, *avr-14B* gene expression was 1.60 times higher in worms from the resistant isolate than in worms from a susceptible isolate, and in females it was 1.43 times higher. However, these differences between the sexes did not prove to be statistically significant (Fig. 2B). The higher constitutive transcription in female compared to males could be due to the contribution of eggs in the female reproductive system. Although the up-regulation of the *avr-14B* gene was described in larvae of both resistant isolates, the differences were not sufficiently great to consider *avr-14B* to be the sole or even a major determinant of IVM resistance in *T. circumcincta*. More isolates would need to be studied to come to such a conclusion. Contrary to the results presented here, in *C. oncophora*, the transcription level of this subunit in L3, adult male and adult female worms showed significantly lower levels in resistant worms

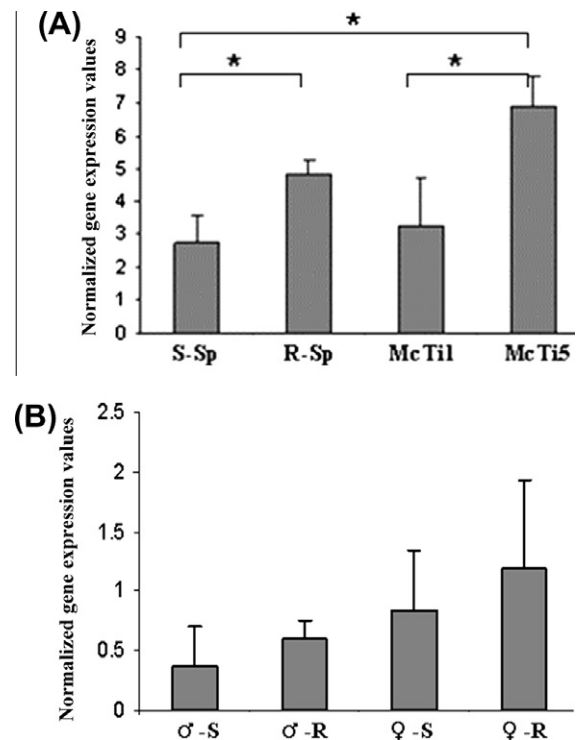


Fig. 2. RT-PCR from the susceptible and resistant *T. circumcincta* populations. A: Analysis of L3 from the Scottish and Spanish populations. B: Analysis of male/female adult worms from the Spanish population. Significant differences ( $p < 0.05$ ) are indicated with \*.

compared with susceptible ones (El-Abdellati et al., 2011). Similar results were obtained with adult *O. ostertagi* worms (El-Abdellati et al., 2011). Transcriptional down-regulation has been also reported recently as a possible resistance mechanism in nicotinic acetylcholine receptor subunits from *Ancylostoma caninum* worms with pyrantel resistance (Kopp et al., 2009). However, in a field isolate of resistant *H. contortus*, Hejmadi et al. (2000) found no changes in channel expression of the subunits HG2, HG3 and HG4 using subunit-specific antibodies. The up-regulation of the gene encoding the avr-14B subunit in the *T. circumcincta* isolates examined in the present study could be influenced not only by IVM resistance but also by co-selection with other anthelmintics, since multiple resistance was described for both resistant isolates. A much more significant increase in expression level (approximately 50-fold) was recently reported in a *T. circumcincta* p-glycoprotein homologue (Tci-pgp-9) when comparing susceptible and resistant isolates, specifically MTci5 (Dicker et al., 2011), hence p-glycoproteins may be more convincing candidate IVM resistance genes.

The results of the present study cannot unequivocally prove a link between avr-14B and IVM resistance either through analysis of sequence polymorphism or expression levels, but a genetic effect could be present in the vicinity of this gene. IVM resistance is proposed to be a multigenic phenomenon (Le Jambre et al., 1999) and the present study would suggest that, if the avr-14B subunit is involved in IVM resistance in *T. circumcincta*, its role is probably relatively minor.

## Acknowledgements

This study has been funded by the national projects INIA-MEC, RTA2006-00183-C03-02 and RTA2010-00094-C03-02. The work of María Martínez-Valladares has been supported by a postdoctoral Jae-Doc contract from the Consejo Superior de Investigaciones Científicas (CSIC) and co-funded by the European Social Fund. The authors would also like to thank Dr. Jeff Eng, McGill University, Montreal, QC for his help with the SSCP analysis and Dr Fiona Kenyon of the Moredun Research Institute, Edinburgh, for her help with the LFIA analysis. The financial support of the Scottish Government Rural and Environmental Research and Analysis Directorate (RERAD) is gratefully acknowledged.

## Appendix A. Supplementary data

Supplementary data associated with this article can be found, in the online version, at <http://dx.doi.org/10.1016/j.ijpddr.2012.03.005>.

## References

- Álvarez-Sánchez, M.A., Pérez-García, J., Bartley, D., Jackson, F., Rojo-Vázquez, F.A., 2005. The larval feeding inhibition assay for the diagnosis of nematode anthelmintic resistance. *Exp. Parasitol.* 110, 56–61.
- Bartley, D.J., Jackson, F., Jackson, E., Sargison, N., 2004. Characterisation of two triple resistant field isolates of *Teladorsagia* from Scottish lowland sheep farms. *Vet. Parasitol.* 123, 189–199.
- Blackhall, W.J., Pouliot, J.F., Prichard, R.K., Beech, R.N., 1998. *Haemonchus contortus*: selection at a glutamate-gated chloride channel gene in ivermectin- and moxidectin-selected strains. *Exp. Parasitol.* 90, 42–48.
- Blackhall, W.J., Prichard, R.K., Beech, R.N., 2008. P-glycoprotein selection in strains of *Haemonchus contortus* resistant to benzimidazoles. *Vet. Parasitol.* 152, 101–117.
- Blaxter, M.L., De Ley, P., Garey, J.R., Liu, L.X., Scheldeman, P., Vierstraete, A., Vanfleteren, J.R., Mackey, L.Y., Dorris, M., Frisse, L.M., Vida, J.T., Thomas, W.K., 1998. A molecular evolutionary framework for the phylum Nematoda. *Nature* 392, 71–75.
- Büttner, C., Sadtler, S., Leyendecker, A., Laube, B., Griffon, N., Betz, H., Schmalzing, G., 2001. Ubiquitination precedes internalization and proteolytic cleavage of plasma membrane-bound glycine receptors. *J. Biol. Chem.* 276, 42978–42985.
- Cully, D.F., Vassilatis, D.K., Liu, K.K., Pares, P.S., Van der Ploeg, L.H., Schaeffer, J.M., Arena, J.P., 1994. Cloning of an ivermectin-sensitive glutamate-gated chloride channel from *Caenorhabditis elegans*. *Nature* 371, 707–711.
- Dent, J.A., Davis, M.W., Avery, L., 1997. Avr-15 encodes a chloride channel subunit that mediates inhibitory glutamatergic neurotransmission and ivermectin sensitivity in *Caenorhabditis elegans*. *EMBO J.* 16, 5867–5879.
- Dent, J.A., Smith, M.M., Vassilatis, D.K., Avery, L., 2000. The genetics of ivermectin resistance in *Caenorhabditis elegans*. *Proc. Natl. Acad. Sci. USA* 97, 2674–2679.
- Dicker, A.J., Nisbet, A.J., Skuce, P.J., 2011. Gene expression changes in a p-glycoprotein (Tci-pgp-9) putatively associated with ivermectin resistance in *Teladorsagia circumcincta*. *Int. J. Parasitol.* 41, 935–942.
- El-Abdellati, A., De Graef, J., Van Zeveren, A., Donnan, A., Skuce, P., Walsh, T., Wolstenholme, A., Tait, A., Vercauteren, J., Claerebout, E., Geldhof, P., 2011. Altered avr-14B gene transcription patterns in ivermectin-resistant isolates of the cattle parasites, *Cooperia oncophora* and *Ostertagia ostertagi*. *Int. J. Parasitol.* 41, 951–957.
- Fucile, S., De Saint Jan, D., de Carvalho, L.P., Bregestovski, P., 2000. Fast potentiation of glycine receptor channels of intracellular calcium in neurons and transfected cells. *Neuron* 28, 571–583.
- geNorm manual, update July 8, 2008. <<http://www.medgen.ugent.be/~jvdesomp/genorm/>>.
- Ghosh, R., Andersen, E.C., Shapiro, J.A., Gerke, J.P., Kruglyak, L., 2012. Natural variation in a chloride channel subunit confers ivermectin resistance in *C. elegans*. *Science* 335, 574–578.
- Harvey, R.J., Depner, U.B., Wässle, H., Ahmadi, S., Heindl, C., Reinold, H., Smart, T.G., Harvey, K., Schütz, B., Abo-Salem, O.M., Zimmer, A., Poisbeau, P., Welzl, H., Wolfer, D.P., Betz, H., Zeilhofer, H.U., Müller, U., 2004. GlyR alpha3: an essential target for spinal PGE2-mediated inflammatory pain sensitization. *Science* 7, 884–887.
- Hejmadi, M.V., Jagannathan, S., Delany, N.S., Coles, G.C., Wolstenholme, A.J., 2000. l-glutamate binding sites of parasitic nematodes: an association with ivermectin resistance? *Parasitology* 120, 535–545.
- Hibbs, R.E., Gouaux, E., 2011. Principles of activation and permeation in an anion-selective Cys-loop receptor. *Nature* 474, 54–60.
- Horozok, L., Raymond, V., Sattelle, D.B., Wolstenholme, A.J., 2001. GLC-3: a novel fipronil and BIDN-sensitive, but picrotoxinin-insensitive, l-glutamate-gated chloride channel subunit from *Caenorhabditis elegans*. *Br. J. Pharmacol.* 132, 1247–1254.
- Jagannathan, S., Laughton, D.L., Critten, C.L., Skinner, T.M., Horozok, L., Wolstenholme, A.J., 1999. Ligand-gated chloride channel subunits encoded by the *Haemonchus contortus* and *Ascaris suum* orthologues of the *Caenorhabditis elegans* gbr-2 (avr-14) gene. *Mol. Biochem. Parasitol.* 103, 129–140.
- Kaminsky, R., Mosimann, D., Sager, H., Stein, P., Hosking, B., 2009. Determination of the effective dose rate for monepantel (AAD 1566) against adult gastrointestinal nematodes in sheep. *Int. J. Parasitol.* 39, 443–446.
- Kopp, S.R., Coleman, G.T., Traub, R.J., McCarthy, J.S., Kotze, A.C., 2009. Acetylcholine receptor subunit genes from *Ancylostoma caninum*: altered transcription patterns associated with pyrantel resistance. *Int. J. Parasitol.* 39, 435–441.
- Laughton, D.L., Lunt, G.G., Wolstenholme, A.J., 1997. Alternative splicing of a *Caenorhabditis elegans* gene produces two novel inhibitory amino acid receptor subunits with identical ligand binding domains but different ion channels. *Gene* 201, 119–125.
- Le Jambre, L.F., Lenane, I.J., Wardrop, A.J., 1999. A hybridisation technique to identify anthelmintic resistance genes in *Haemonchus*. *Int. J. Parasitol.* 29, 1979–1985.
- Martínez-Valladares, M., Famularo, M.R., Fernández-Pato, N., Cordero-Pérez, C., Castañón-Ordóñez, L., Rojo-Vázquez, F.A., 2012. Characterization of a multidrug resistant *Teladorsagia circumcincta* isolate from Spain. *Parasitol. Res.* 110, 2083–2087.
- McCavera, S., Walsh, T.K., Wolstenholme, A.J., 2007. Nematode ligand-gated chloride channels: an appraisal of their involvement in macrocyclic lactone resistance and prospects for developing molecular markers. *Parasitology* 134, 1111–1121.
- McCavera, S., Rogers, A.T., Yates, D.M., Woods, D.J., Wolstenholme, A.J., 2009. An ivermectin-sensitive glutamate-gated chloride channel from the parasitic nematode *Haemonchus contortus*. *Mol. Pharmacol.* 75, 1347–1355.
- Mes, T.H., 2004. Purifying selection and demographic expansion affect sequence diversity of the ligand-binding domain of a glutamate-gated chloride channel gene of *Haemonchus placei*. *J. Mol. Evol.* 58, 466–478.
- Njue, A.I., Hayashi, J., Kinne, L., Feng, X.P., Prichard, R.K., 2004. Mutations in the extracellular domains of glutamate-gated chloride channel alpha3 and beta subunits from ivermectin-resistant *Cooperia oncophora* affect agonist sensitivity. *J. Neurochem.* 89, 1137–1147.
- Njue, A.I., Prichard, R.K., 2004. Genetic variability of glutamate-gated chloride channel genes in ivermectin-susceptible and -resistant strains of *Cooperia oncophora*. *Parasitology* 129, 741–751.
- Prichard, R., 1994. Anthelmintic resistance. *Vet. Parasitol.* 54, 259–268.
- Sadtler, S., Laube, B., Lashub, A., Nicke, A., Betz, H., Schmalzing, G., 2003. A basic cluster determines topology of the cytoplasmic M3–M4 loop of the glycine receptor alpha1 subunit. *J. Biol. Chem.* 278, 16782–16790.
- Skuce, P., Stenhouse, L., Jackson, F., Hypps, V., Gilleard, J., 2010. Benzimidazole resistance allele haplotype diversity in United Kingdom isolates of *Teladorsagia circumcincta* supports a hypothesis of multiple origins of resistance by recurrent mutation. *Int. J. Parasitol.* 40, 1247–1255.
- Tandon, R., LePage, K.T., Kaplan, R.M., 2006. Cloning and characterization of genes encoding alpha and beta subunits of glutamate-gated chloride channel protein in *Cylicocyclus nassatus*. *Mol. Biochem. Parasitol.* 150, 46–55.

- Thompson, A.J., Lester, H.A., Lummis, S.C., 2010. The structural basis of function in Cys-loop receptors. *Q. Rev. Biophys.* 43, 449–499.
- Vandesompele, J., De Preter, K., Pattyn, F., Poppe, B., Van Roy, N., De Paepe, A., Speleman, F., 2002. Accurate normalization of real-time quantitative RT-PCR data by geometric averaging of multiple internal control genes. *Genome Biol.* 3(7), research/0034.
- Van Zeveren, A.M., Visser, A., Hoorens, P.R., Vercruyse, J., Claerebout, E., Geldhof, P., 2007. Evaluation of reference genes for quantitative real-time PCR in *Ostertagia ostertagi* by the coefficient of variation and geNorm approach. *Mol. Biochem. Parasitol.* 153, 224–227.
- Wolstenholme, A.J., Fairweather, I., Prichard, R., von Samson-Himmelstjerna, G., Sangster, N.C., 2004. Drug resistance in veterinary helminths. *Trends Parasitol.* 20, 469–476.
- Yates, D.M., Wolstenholme, A.J., 2004. An ivermectin-sensitive glutamate-gated chloride channel subunit from *Dirofilaria immitis*. *Int. J. Parasitol.* 34, 1075–1081.